

# Design and Implementation of a Low Cost, Pump-Based, Depth Control of a Small Robotic Fish

Michail Makrodimitris, *Student Member, IEEE*, Ioannis Aliprantis and  
Evangelos Papadopoulos, *Senior Member, IEEE*

**Abstract**— Recently, there has been growing interest in biomimetic underwater vehicles. To exploit the full workspace of this kind of vehicles, depth control is needed and plays a critical role. Although depth control for large vehicles such as submarines has been addressed, this issue for low-cost, small-scale underwater vehicles has not received attention. In this paper, the depth control of a small robotic fish is studied, and implemented with the use of a small dc pump. The depth system dynamics are developed and limitations arising from the low-cost, small-scale actuators and sensors are described. A controller with limited feedback is designed, implemented and validated both by simulations and experiments. It is expected that this controller will add an important dimension to depth control of low-cost, energy-efficient small underwater vehicles.

## I. INTRODUCTION

Depth control of underwater vehicles is an important issue in underwater robotic systems. Without depth control, the full workspace of underwater vehicles cannot be utilized. Until recently, researchers have seen depth control as an issue associated with large underwater vehicles such as submarines or Autonomous Underwater Vehicles (AUV) [1]. Vehicles of this type change their buoyancy usually using ballast tanks (MBTs, DCTs), which can be filled with seawater in order to submerge, or pressurized air in order to surface. In small Remotely Operated Vehicles (ROV), depth control is often achieved with the help of thrusters. However, many hypotheses regarding the vertical control of submarines appear to be questionable, when one tries to implement the same depth control techniques in smaller scales and with low cost, because thruster mechanisms are bulky and consume a lot of energy. In addition, they are not acceptable in the design of biomimetic vehicles, as thrusters annoy fish populations and cannot be used to monitor them.

Various control approaches have been proposed. For example, Maalouf et al., investigated differences between PD control and nonlinear adaptive control of a tethered AUV [2]. However, a common characteristic in similar research works, is that they are based on simulations. Preliminary work was carried out applying the well-known control method of LQR [3], [4]. However, these methods have high

computational requirements and require substantial computing power, exceeding that found in microcontrollers.

In nature, fish control their depth with different approaches. Sharks, for example, use dynamic lift to maintain or change their depth, by changing the angle of their pectoral fins [5]. Other species change their depth, by means of a gas bladder or by storing oils and lipids.

In biomimetics, depth control can be achieved with the help of mechanical pectoral fins, by controlling their angles [6], [7]. However, this approach has the disadvantage that sinking or rising is impossible at zero or very low velocities. Other methods for controlling the depth of robotic fish, such as the one shown in Fig. 1, include the use of small motors, pistons, ballast tanks and small pumps.

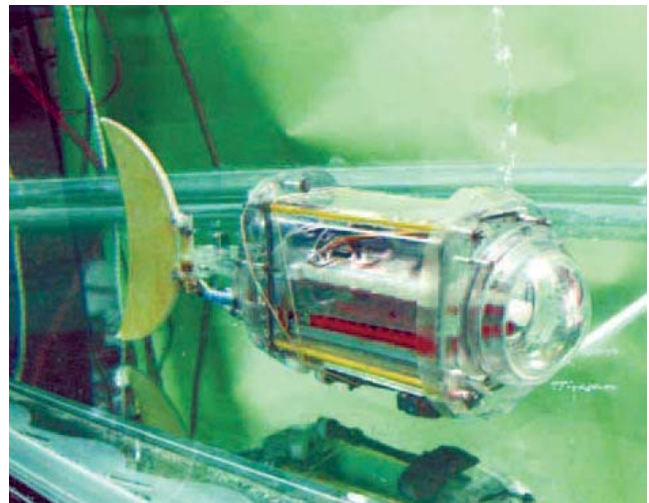


Fig. 1. The robotic fish at the National Technical University of Athens.

A piston-like, screw-based system to displace water was used in [8] and [9]. Although this is an inexpensive solution, the resulting response is very slow. Other researchers tried to imitate the way some whales dive into water, see for example Inoue et al., [10]. The suggested setup is partially impractical for small vehicles, as extra heating and cooling mechanisms of the oil used must be implemented. A combination of foils with a ballast tank was employed in [11]. Although the motion of the foil is quite natural, it is also energy demanding, as a number of motors are required to implement this method. A small number of studies have been carried out, which use small pumps, in order to control the depth of an underwater vehicle, either combined with thrusters [12], or combined with pectoral fins [13]. The use of a small pump employed to change the location of the center of the gravity in small underwater vehicles, and

---

Michail Makrodimitris, Ioannis Aliprantis and Evangelos Papadopoulos are with the Department of Mechanical Engineering, National Technical University of Athens (NTUA), Greece (phone: +30-210-772-3512, 1440; fax: +30-210-772-1450; e-mail: egpapado@central.ntua.gr, mmakrod@mail.ntua.gr, mc08679@central.ntua.gr).

therefore allow for changing their depth, was demonstrated in [14]. This method also cannot produce a lift force when the vehicle is still or moves slowly. Finally, the concept of using artificial muscles driven by small direct current (DC) pumps to power tails was presented in [15]. In terms of control algorithms, all these works in biomimetics use fuzzy, on-off, or PID controllers to regulate the position of pectoral fins and therefore the depth of the vehicle [16].

The aim of this work is to develop a methodology for controlling the depth of small underwater vehicles, at minimum cost. To the best of our knowledge, there is no other work focusing on depth control of a robotic fish, using a small DC pump and a rubber bladder, and on developing a gain-tuning methodology, for use with partial state feedback control. The depth control system dynamics are developed and limitations arising from the low-cost, small-scale actuators and sensors are described. A controller with limited feedback is designed, implemented and validated both by simulations and experiments. As implemented, the controller represents a simple, but interesting solution, in terms of a minimum overhead. More importantly, it achieves its task with simple means.

## II. SYSTEM MODELING

### A. System Model for Control Purposes

The aim of this work was to develop a depth control system for a small robotic fish, which would be able to change its depth quickly, even if the robotic fish would stand still, as some fish are capable of doing. Due to their high-energy consumption and incompatibility with fish populations, thrusters were not considered. Also, pectoral fins cannot change depth at zero velocity and also were not selected. Instead, we opted for a small, brushed DC motor water pump to draw water into or expel water from a bladder within the fish, thus allowing the robotic fish to sink or rise, respectively.

The equations of motion of the vertical motion of the robotic fish are developed next. It is assumed though, that no roll or pitch moments during depth changes occur. Using the linear graph methodology, see Fig. 2, [17], the dynamics of a DC motor driven water pump is given by:

$$J \cdot \dot{\omega}_j + \frac{k_\tau^2 + B_r \cdot R}{R} \cdot \omega_j = -\frac{k_\tau}{R} \cdot V_s - D \cdot P_s \quad (1)$$

The water mass flow of the pump  $q_\mu$  [kg/s], is related to the angular velocity of the pump rotor  $\omega_j$  [rad/s], by the following equation:

$$\omega_j = -\frac{1}{\rho \cdot D} \cdot q_\mu \quad (2)$$

Thus, equation (1) transforms to:

$$\frac{J}{\rho \cdot D} \cdot \dot{q}_\mu + \frac{k_\tau^2 + B_r \cdot R}{R \cdot \rho \cdot D} \cdot q_\mu = \frac{k_\tau}{R} \cdot V_s + D \cdot P_s \quad (3)$$

where  $J$  is the total inertia of the DC motor rotor, the pump's gears, the water and the axes [Kg·m<sup>2</sup>],  $\rho$  the density of the water [kg/m<sup>3</sup>],  $D$  the displacement of the pump [m<sup>3</sup>/rad], and  $P_s$  is the external pressure due to the

water column [N/m<sup>2</sup>]. The coefficients:  $R$  [Ω],  $k_\tau$  [N·m/A],  $V_s$  [Volt] and  $B_r$  [N·s] are the resistance, the torque constant, the voltage and the dynamic friction coefficient of the DC motor. Because the water tank has a depth equal of 80 cm, it is safe to assume that the pressure  $P_s$  does not correlate significantly to the depth in which our fish swims.

Equation (3) may be written, in the simpler form of:

$$\underbrace{\left( \frac{J \cdot R}{k_\tau^2 + B_r \cdot R} \right)}_{\tau} \cdot \dot{q}_\mu + q_\mu = \underbrace{\left( \frac{k_\tau \cdot \rho \cdot D}{k_\tau^2 + B_r \cdot R} \right)}_k \cdot V_s \quad (4)$$

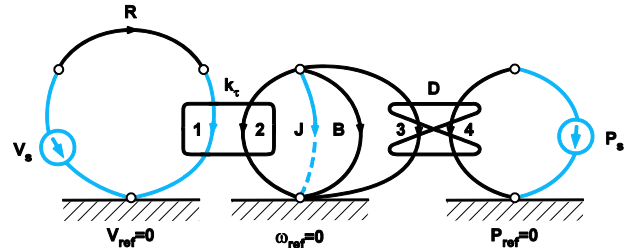


Fig. 2 Linear Graph of the pump's model. The normal tree is in blue.

where  $\tau$  is a time constant and  $k$  a control input constant. As can be seen in (4), these constants incorporate a number of system parameters. Applying Newton's second law and assuming: (a) initial neutral buoyancy of the fish, (b) a single rigid body, and (c) linear vertical drag, a simple model for the vertical motion of the robotic fish is,

$$M \cdot \dot{v} + B \cdot v = g \cdot \mu \quad (5)$$

where  $M$  [kg] is the mass of the robotic fish,  $v$  [m/s] is its vertical velocity,  $B$  [N·s/m] is the linear drag coefficient, computed as a linear fit on the experimental drag force curve for the range of vertical speeds up to 0.14 m/s,  $\mu$  [kg] the variable water mass pumped inside the bladder and  $g$  [m/s<sup>2</sup>] is the acceleration of gravity.

Combining (4) and (5), the open loop depth dynamics of the robotic fish are obtained:

$$\left\{ \begin{array}{l} \dot{q}_\mu = -\frac{q_\mu}{\tau} + \frac{k}{\tau} \cdot V_s \\ \dot{\mu} = q_\mu \\ \dot{v} = -\frac{B}{M} \cdot v + \frac{g}{M} \cdot \mu \\ \dot{h} = v \end{array} \right. \quad (6)$$

where  $h$  [m] is the depth of the robotic fish. Equation (6) can be rewritten in a state variable matrix form:

$$\underbrace{\begin{bmatrix} \dot{q}_\mu \\ \dot{\mu} \\ \dot{v} \\ \dot{h} \end{bmatrix}}_{\dot{x}} = \underbrace{\begin{bmatrix} -\frac{1}{\tau} & 0 & 0 & 0 \\ 1 & 0 & 0 & 0 \\ 0 & \frac{g}{M} & -\frac{B}{M} & 0 \\ 0 & 0 & 1 & 0 \end{bmatrix}}_A \cdot \underbrace{\begin{bmatrix} q_\mu \\ \mu \\ v \\ h \end{bmatrix}}_x + \underbrace{\begin{bmatrix} \frac{k}{\tau} \\ 0 \\ 0 \\ 0 \end{bmatrix}}_B \cdot \underbrace{V_s}_u \quad (7)$$

As it can be easily shown with the help of the parameter values in Table I, the open loop system is controllable.

TABLE I  
SYSTEM PARAMETERS

Symbol	Quantity	Value	Unit
$M$	Mass of fish	0.8515	kg
$\tau$	Time constant	0.2	s
$k$	Control input constant	0.00386	kg/Vs
$g$	Acceleration of gravity	9.81	m/s <sup>2</sup>
$B$	Linear drag coefficient	0.7	Ns/m

### B. Truth Model for Simulations / Evaluation

Although the above model describes the system quite accurately, the real system is much more complicated, thus more difficult to solve. A second, more detailed model for simulation was designed, taking into consideration several nonlinearities of the real system.

Firstly, the selected pump is a low quality component. It is characterized by a complicated nonlinear behavior. One of these characteristics is that it includes a dead zone, as it needs at least 0.7 volt to start. To compensate for this nonlinearity, an offset nonlinearity is added to the controller. Also, the pump operates inefficiently due to water leakage, especially when the pump's rotor is not moving, and exhibits variations in the flow rate, depending on the direction of the rotor. The above characteristics were not simulated to minimize complexity.

Secondly, a saturation block was added before the voltage input of the pump in order to model the limited output voltage (6.5 V) of the H-bridge used. In addition, the pressure sensor returns noisy feedback. This noise was included in the simulation model as a white noise block.

### III. CONTROL DESIGN

Our aim was to develop a simple, and computationally efficient controller. Therefore, minimal feedback and algorithm complexity was preferable. A computationally reasonable algorithm is the full state feedback:

$$V_s = K_e \cdot (h_{des} - h) - K_v \cdot v - K_\mu \cdot \mu - K_{q_\mu} \cdot q_\mu \quad (8)$$

where  $h_{des}$  the desired depth of the fish, and  $K_e, K_{q_\mu}, K_v, K_\mu$  the gains of full state variable control. In (8), the input is the desired depth  $h_{des}$ . Fig. 3 illustrates the state feedback control algorithm in a block diagram form:

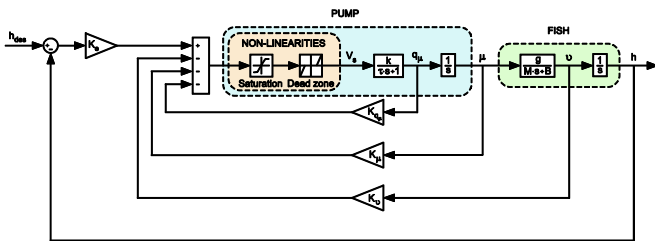


Fig. 3. Block diagram of state feedback depth control.

This controller requires measurement of the depth  $h$ , which

can be provided by the pressure sensor. It also requires feedback of the variable water mass  $\mu$  in the bladder, which in principle can be achieved using an incremental encoder on the pump motor and (2). Then, their derivatives,  $v$  and  $q_\mu$ , can be numerically calculated. Thus with an appropriate gain selection, this controller should produce the desired voltage input to the actuator – the dc water pump.

To keep computational requirements of the controller to a minimum, it is desirable to feed back a minimum set of state variables. However, by reducing the feedback to the two states  $h, v$ , the response deteriorates and this is intensified by the nonlinear system behavior.

To avoid this problem, we opted for a three state variable feedback, achieved by setting  $K_\mu = 0$ . This choice results in a controller that feeds back the mass flow of the water in the bladder  $q_\mu$ , the height  $h$  and the vertical velocity  $v$  of the robotic fish. The feasibility of this choice was confirmed by using the Routh-Hurwitz stability criterion, which showed that the required stability conditions are all satisfied; i.e. when  $K_\mu = 0$ , all coefficients in the denominator of (9) are positive, etc. By substituting the system parameters, given in Table I, the closed loop transfer function of the system is,

$$\frac{h(s)}{h_{des}(s)} = \frac{1}{a_4 \cdot s^4 + \alpha_3 \cdot s^3 + \alpha_2 \cdot s^2 + \alpha_1 \cdot s + 1} \quad (9)$$

where the coefficients  $\alpha_4, \alpha_3, \alpha_2, \alpha_1$  are functions of the gains and are given in the Appendix. Combining the transfer function in (9) with the rules of Root Locus, a valid set of gains is selected as:  $K_e = 5.4$ ,  $K_{q_\mu} = 500$ ,  $K_v = 30$ . Due to the corresponding pole location, it is expected that this set of gains will yield a fast response with minimum oscillations.

However, in practice the response will be subject to nonlinearities and limitations, and therefore, one should have guidelines as to what happens when the control gains are fine-tuned around the nominal design. To obtain such guidelines, the characteristic equation was put in the form of root-locus equations for each gain of interest:

$$1 + K_e \cdot \frac{1}{4.497 \cdot s^4 + 69.58 \cdot s^3 + 54.16 \cdot s^2 + 30 \cdot s} = 0 \quad (10)$$

$$1 + K_v \cdot \frac{0.185 \cdot s}{0.8328 \cdot s^4 + 12.89 \cdot s^3 + 10.03 \cdot s^2 + 1} = 0 \quad (11)$$

$$1 + K_{q_\mu} \cdot \frac{0.016 \cdot s^3 + 0.013 \cdot s^2}{0.833 \cdot s^4 + 4.849 \cdot s^3 + 3.423 \cdot s^2 + 5.556 \cdot s + 1} = 0 \quad (12)$$

Figure 4, illustrates the system behavior in the case of changing each gain independently. In this figure only the dominant poles of the system are shown. As one can see from this figure, if gain  $K_e$  increases, the system becomes unstable. If the value of  $K_{q_\mu}$  decreases or  $K_v$  increases, respectively, the response is a little faster according to the desired depth, but the amplitude of the oscillations increases as well. The figure also shows the necessity for a tuning methodology. Since there are poles close to the imaginary axis, resulting in oscillations, an alternative solution would be to move the system poles of (7) to the left of the imaginary axis, by changing the values of matrix A, i.e. by changing the fish design. However, this is a line of research that will be explored in the future.

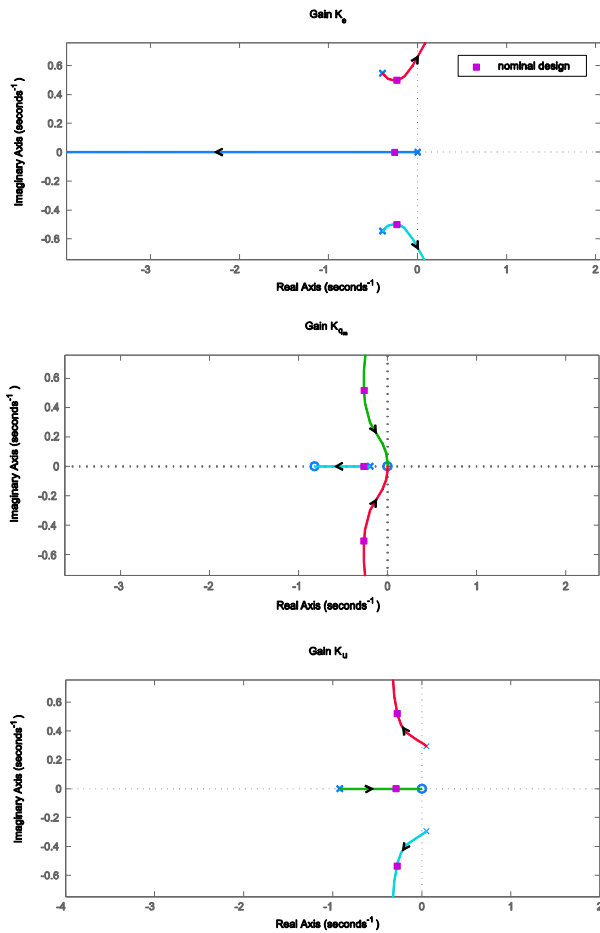


Fig. 4. Root Locus for gains  $K_c$ ,  $K_v$ ,  $K_u$ . Arrows show increasing gain.

#### IV. IMPLEMENTATION

Our experimental setup, used to validate our design, consists of a water tank with a towing mechanism on top and a robotic fish. The dimensions of our robotic fish are 30 cm (L) x 8 cm (W) x 7 cm (H). Due to space limitations, the experimental tank size had to be constrained by 5 m (L) x 1 m (W) x 0.8 m (H), see Fig. 5.

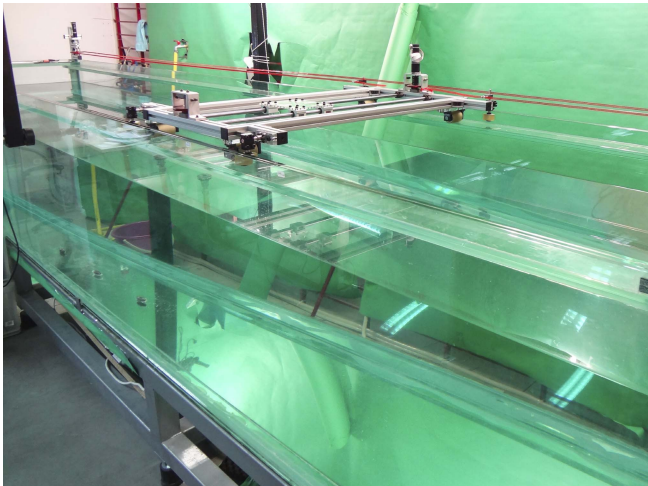


Fig. 5. The CSL-NTUA experimental tank used in our experiments.

#### A. Hardware Implementation of Robotic Fish

The depth control module consists of the following modules:

(a) For controlling the robotic fish a low cost, 8-bit PIC18F4431 Microchip microcontroller was used. It has a module to decode quadrature signal, which is important in order to receive data from the incremental encoder. It can be easily programmed in C, and can use frequency quartz crystals up to 40 Mhz. Fig. 6 illustrates the system main hardware components.

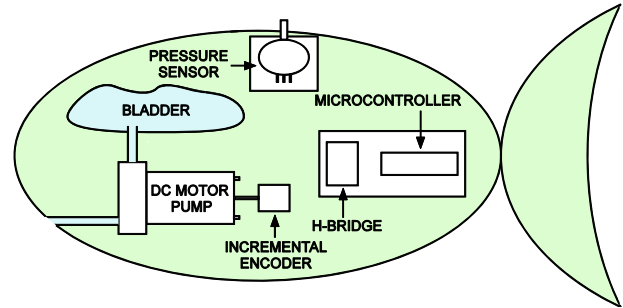


Fig. 6. Hardware setup of robotic fish.

(b) A critical step was to select a DC water pump, which would satisfy our specifications. These included: (i) small, in order to fit inside the robotic fish, (ii) of low cost, (iii) two-directional, (iv) low DC voltage to match the available battery cells. Additionally, it should yield enough flow rate, capable of a low response time. After a thorough market research, the RS-360SH gear water pump was selected, (Fig 7i). The pump is driven by a 40W, 9V DC Mabuchi motor.

(c) In the proposed control scheme a measurement of the variable mass, pumped into the bladder of the robotic fish, was required. For this reason, a HES164A magnetic quadrature incremental encoder was custom fitted to the rotor of the water pump. The encoder on the motor gives 2 pulses per revolution (Fig 7iv).

(d) To ensure a depth feedback in our control algorithm, a gauge piezoresistive pressure transducer was used. The selected pressure sensor is the Freescale MPX5010GP (Fig 7iii). These sensors are designed for a wide range of applications, particularly those employing a microcontroller or microprocessor with A/D inputs. These sensors provide an accurate high-level analog output signal that is proportional to the applied pressure. They are temperature-compensated and their response is almost linear. The pressure sensors voltage output range between 0.2 and 4.7 V, for pressure inputs in the range of 0-1 bar, respectively. The correlation between voltage outputs of the pressure sensor and the depth of the fish was identified with a polynomial, experimentally.

(e) The H-bridge should at minimum meet the 6.5 V, 2 A requirements. An inexpensive and robust choice is the MC33926. Output loads can be pulse-width-modulated at frequencies up to 20 kHz with peak currents up to 5 A. This H-bridge has TTL/CMOS logic compatible inputs, which makes it easy to be integrated with a microcontroller. The H-Bridge has also a load current feedback feature (Fig 7ii).

(f) As a bladder, a big rubber balloon was used.

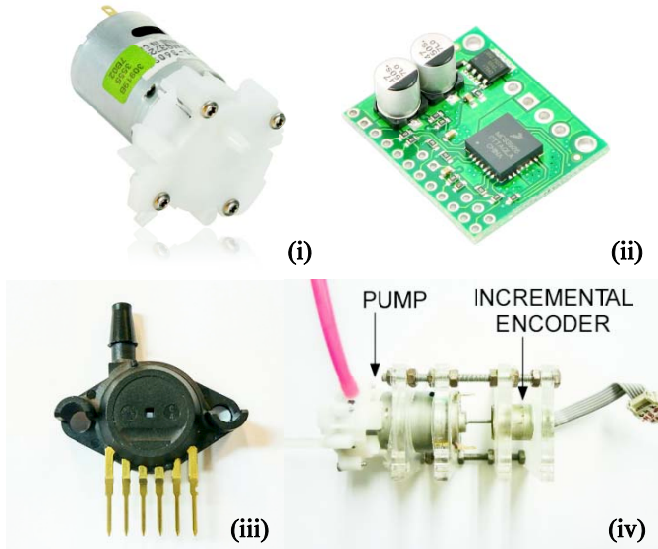


Fig. 7. Depth control hardware parts: (i) DC water pump, (ii) H-bridge (iii) pressure sensor, (iv) incremental encoder attached to pump.

### B. Software Design

The toolchain utilized to program the microcontrollers included the following: MPLAB v.8, C18 Microchip compiler and MPLAB ICD2. Software was written in C, due to the large availability of relative compilers and necessary software libraries. The program running on our microcontroller starts with an auto-calibration routine of the pressure sensor. A 10-bit ADC conversion provides voltages from the pressure sensor every 50  $\mu$ s. Because the measurements were noisy, an average of the data, was implemented every 10 samples, in addition to a low-pass filter, resulting in a remarkable reduction of signal noise.

Time scheduling is executed with the help of interrupt driven, real-time timers. In addition, data is received from the encoder. The closed loop control is executed every 25 ms, which is in accordance with the Nyquist Theorem and the slow dynamics of the robotic fish along the vertical axis.

By knowing the counts sent by the incremental encoder, and through the application of numerical techniques, the angular velocity of the pump can be computed. This real-time calculation was a strenuous task, because of the noise and errors in measurements, due to the pressure sensor and the incremental encoder.

An approach that worked well was that of using four successively averaged measurements of each sensor:

$$\omega_j = \frac{\theta(t) + 3 \cdot \theta(t - \Delta T) - 3 \cdot \theta(t - 2\Delta T) - \theta(t - 3\Delta T)}{6\Delta T} \quad (13)$$

The above definition of the first derivative was also used to provide the velocity of the robotic fish from the depth measurements of the pressure sensor, as it further reduces measurement noise.

As mentioned earlier, the controller uses an offset block to compensate for pump dead zone nonlinearities. The pseudocode algorithm for the offset compensation in the controller is the following:

```
if(controller output >= 0){
```

```
    controller output = controller output + 0.7;
}
if(controller output < 0){
    controller output = - controller output;
    controller output = -( controller output + 0.7);
}
```

Lastly, during the experiments, all data were saved in real time in an external memory and were received afterwards offline through SPI protocol and a serial port.

## V. RESULTS

### A. Simulation Results

The depth control of the robotic fish was validated using the developed truth model in MATLAB. The model that was simulated was that of Fig. 3 (with  $K_\mu = 0$ ), in addition to a dead zone model, an H-bridge saturation block and the above mentioned, dead zone compensator for the water pump. Two simulations were performed. The first simulation was carried out without quantization error and sensor noise; while in the second one, additive sensor in the form of white noise was used. The results from both are depicted in Fig. 8 for a desired depth of 0.2 m. As can be seen, the oscillation in steady state with noise has amplitude just below  $\pm 2$  cm and an offset of about -1 cm.

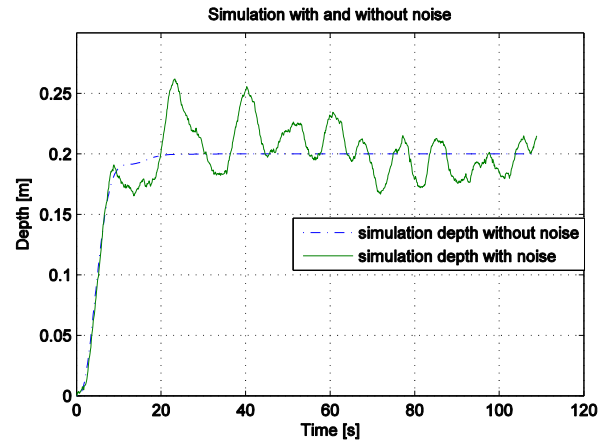


Fig. 8. Simulated Depth response comparison without and with noise.

### B. Experimental Results

The setup used in the experiments has been described briefly in Section IV. The experiment is conducted in the following way: First, the desired depth input (0.2 m) is transmitted to the microcontroller. Then, we placed the robotic fish in the water. The initial water mass in the bladder must be carefully set, in order to ensure neutral buoyancy. The outcome of the experiments compared to the simulation without noise, is shown in Fig. 9.

Comparing simulation and experimental results, Figs. 8 and 9, one may say that there is a satisfactory agreement between the simulation and experiments. The observed oscillations can be explained as follows:

(i) An inexpensive pressure sensor was used. By using a better pressure sensor, as the simulation in Fig 8 showed, the response would improve.

(ii) The dominant poles of the model were near the imaginary axes primarily due to fish design. Some oscillations were therefore expected. However, due to the methodology used, the depth was stabilized and the oscillations were minimized within  $\pm 2$  cm.

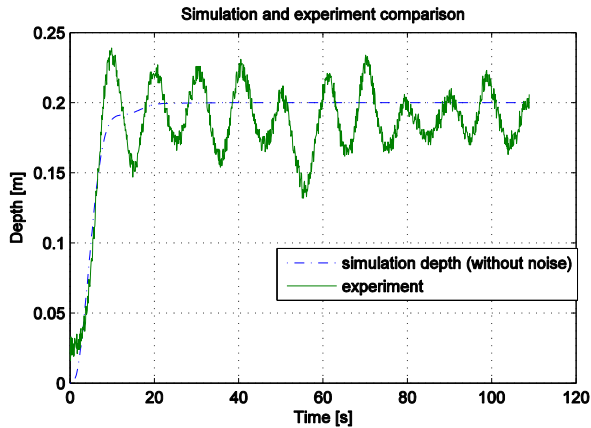


Fig. 9. Experimental depth response compared with the ideal noiseless simulated response.

#### CONCLUSION

In this paper, the depth control of a small robotic fish, with the help of a small dc pump, was studied. The encountered challenges were presented, due to the usage of low quality, small-scaled components and their solutions. A system model, as well as a closed loop, reduced state variable controller, was suggested. A hardware design was implemented and thoroughly explained. This model was validated by comparison with both simulation and experimental measurements. Both simulation and experimental data were in good agreement. We think that the new model can be used to control, successfully, the depth of any low-cost, energy efficient small underwater vehicle.

#### APPENDIX

The coefficients of the polynomial in (9) are given below:

$$\alpha_1 = \frac{K_\mu \cdot B + K_v \cdot g}{K_e \cdot g} \quad (A1)$$

$$\alpha_2 = \frac{B + (K_{q_\mu} \cdot B \cdot k) + (K_\mu \cdot M \cdot k)}{K_e \cdot k \cdot g} \quad (A2)$$

$$\alpha_3 = \frac{\tau \cdot B + M + K_{q_\mu} \cdot M \cdot k}{K_e \cdot k \cdot g} \quad (A3)$$

$$\alpha_4 = \frac{\tau \cdot M}{K_e \cdot k \cdot g} \quad (A4)$$

All parameters in (A1)-(A4) are defined in (8) and Table I.

#### REFERENCES

[1] Y. Shawn, A. Woods, Robert J. Bauer, and Mae L. Seto, "Automated Ballast Tank Control System for Autonomous Underwater Vehicles,"

*IEEE Journal of Oceanic Engineering*, Volume 37, Issue 4, August 2012, pp 727-739.

[2] D. Maalouf, I. Tamanaja, E. Campos, A. Chemori, V. Creuze, J. Torres, R. Lozano, "From PD to Nonlinear Adaptive Depth-Control of a Tethered Autonomous Underwater Vehicle," *IFAC Joint Conference 2013, 5th Symposium on System Structure and Control*, Grenoble, France, 2013.

[3] Jeffery S. Riedel, Anthony J. Healey, David B. Marco and Bahadir Beyazay, "Design and Development of Low Cost Variable Buoyancy System for the Soft Grounding of Autonomous Underwater Vehicles," *International Symposium on Unmanned untethered submersible technology*, 1999, p. 427-438.

[4] Maziyah Mat Noh, Mohd Rizal Arshad, Rosmiwati Mohd Mokhtar, "Depth and pitch control of USM underwater glider: performance comparison PID vs. LQR," *Indian Journal of Geo-Marine Sciences (IJMS) NISCAIR-CSIR, India*, Apr. 2011, volume 40, pp. 200-206.

[5] JJ Videler, *Fish Swimming*, 1st Edition, Chapman & Hall, 1993.

[6] Le Zhang, Wei Zhao, Yonghui Hu, Dandan Zhang, and Long Wang, "Development and Depth Control of Biomimetic Robotic Fish," *Proc. IEEE/RSJ International Conference on Intelligent Robots and Systems*, San Diego, CA, USA, Oct 29 - Nov 2, 2007, pp. 3560-3565.

[7] Chuanmeng Niu, Lige Zhang, Shusheng Bi and Yueri Cai, "Development and Depth Control of a Robotic Fish Mimicking Cownose Ray," *Proc. IEEE International Conference on Robotics and Biomimetics*, December 2012, Guangzhou, China, pp. 814-818.

[8] Bambang Sumantri, Karsiti, M.N, "Development of variable ballast mechanism for depth positioning of spherical URV," *International Symposium on ITS Information Technology*, Aug. 2008 Kuala Lumpur, Malaysia, Volume 4, pp.1-6.

[9] Le Minh Thuan, Nguyen Truong Thinh, Nguyen Ngoc Phuong, "Study of Artificial Fish Bladder System for Robot Fish," *Proceedings of the 2011 IEEE International Conference on Robotics and Biomimetics*, December 2011, Phuket, Thailand, pp. 2126-2130.

[10] Tomotaka Inoue, Koji Shibuya and Akinori Nagano, "Underwater Robot with a Buoyancy Control System Based on the Spermacti Oil Hypothesis - Development of the Depth Control System," *IEEE/RSJ, International Conference on Intelligent Robots and Systems (IROS)*, 2010, Taipei, Oct. 2010, pp. 1102-1107.

[11] K.H. Low, "Maneuvering and Buoyancy Control of Robotic Fish Integrating with Modular Undulating Fins," *Proc. IEEE International Conference on Robotics and Biomimetics*, December 17-2, 2006, Kunming, China, p.1012-017.

[12] Carrick Detweiler, Stefan Sosnowski, Iuliu Vasilescu, and Daniela Rus, "Saving Energy with Buoyancy and Balance Control for Underwater Robots with Dynamic Payloads," *Experimental Robotics Springer Tracts in Advanced Robotics*, Volume 54, 2009, pp. 429-438.

[13] Pei-Jun Lee, Meng-Shiue Lee, and Ruei-Chan Wang, "A Fuzzy Control Based Robotic Fish with Multiple Actuators," *International Journal of Fuzzy Systems*, Vol. 14, No. 1, March 2012, pp. 45-53.

[14] Feitian Zhang, John Thon, Cody Thon and Xiaobo Tan, "Miniature Underwater Glider: Design, Modeling, and Experimental Results," *IEEE Int. Conference on Robotics and Automation, (ICRA 2012)*, River Centre, Saint Paul, Minnesota, USA, May 2012, pp. 4904-4910.

[15] Daejung Shin, Seung You Na, Jin Young Kim, Min-Gyu Song, "Development and Performance Analysis of Artificial Muscle for Fish Robots Using Water Pumps," *Third International Conference on Convergence and Hybrid Information Technology*, 2008. ICCIT '08, Busan, Volume 1, pp. 403-408.

[16] Whei Zhao, Junzhi Yu, Yiming Fang, and Long Wang, "Development of Multi-mode Biomimetic Robotic Fish Based on Central Pattern Generator," *Proc. IEEE/RSJ Int. Conference on Intelligent Robots and Systems*, October 9-15, 2006, Beijing, China, p.3891-3896.

[17] Derek Rowell and David N. Wormley, *Introduction to System Dynamics*, 1st Edition, Prentice Hall, 1996.